PERSISTENT MOTION AND CHAOS IN ATTITUDE CONTROL WITH SWITCHING ACTUATORS

Alexandre Rodrigues Mesquita[1]
Karl Heinz Kienitz[2]

[1] *Instituto Tecnológico de Aeronáutica*
12.244-090 São José dos Campos,SP – Brazil

[2] *Institute for Robotics and Mechatronics*
DLR Oberpfaffenhofen, Postfach 11 16, D-82230 Weßling, Germany
(on leave from Instituto Tecnológico de Aeronáutica)

Abstract: In systems with switching actuators persistent motions of different nature may occur, such as limit cycles, quasi-periodic and chaotic motions. In this contribution the nature of persistent motions in an attitude control system with switching actuators subject to switching restrictions are examined as a function of controller parameters. Bifurcation diagrams are used to describe observations. In the light of the bifurcation diagrams, control issues and earlier results obtained with the describing function method are assessed from a more general perspective.

Keywords: Limit cycles; Chaotic behaviour; Switching functions; Attitude control; Nonlinear control systems.

1. INTRODUCTION

Throughout the last decades, attitude control systems with switching actuators have been used in satellite and launching systems (Mendel, 1970; Won, 1999; Oliveira and Kienitz, 2000; Avanzini, 2001). In the attitude stabilization phase, such systems typically have been operated in limit cycle conditions. As shown by Oliveira and Kienitz (2000), non-conventional analysis / design problems arise when actuators are subject to switching-time restrictions. Certain conditions ensure that limit cycles exist. When these conditions do not hold, system motion may not be of limit cycle type.

During recent research on the issue of robust limit cycle control, it was observed that persistent motions of different nature may occur, such as quasi-periodic and chaotic motions. In this contribution the nature of persistent motions in an attitude control system with switching actuators subject to switching restrictions are examined as a function of controller parameters. Bifurcation diagrams are used to describe observations. Bifurcation diagrams are produced with data collected from extensive system simulation. Simulations were performed using a master-slave two PC hardware setup. In the light of the bifurcation diagrams, earlier results obtained with the describing function method are assessed in a more general perspective.

This contribution is structured as follows: in section 2 a problem description is given; section 3 is devoted to delay modelling; section 4 describes simulation strategies used; results are presented in section 5 and conclusions are found in section 6.

2. PROBLEM DESCRIPTION

The problem description given here is akin to that given by Oliveira and Kienitz (2000). Consider a simple rigid body (e.g. satellite or rocket in the upper atmosphere) whose attitude ϕ is to be controlled using sets of small thrusters, which are switching actuators with switching time restrictions. A simplified representation of the system is shown in Fig. 1.

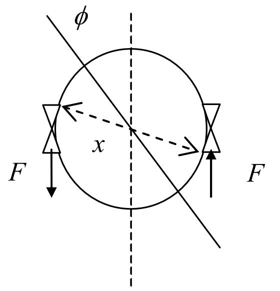

Fig. 1: Rigid body with set of thrusters.

Body inertia of 1500 Nm^2 is given. The small thruster actuators do have delays and switching-time restrictions. Their characteristics are:

- Total maximum moment: 308 Nm
- Delays (when switching on):
  - delay until 10% of thrust: 10 – 30 [ms]
  - delay until 90% of thrust: 20 – 50 [ms]
- Delays (when switching off):
  - delay until 90% of thrust: 9 – 16 [ms]
  - delay until 10% of thrust: 15-50 [ms]
- Switching-time restrictions:
  - duration of pulses (t_{on_min}): > 100 [ms]
  - rest between successive pulses of the same motor: > 50 [ms]
  - rest between switching-off of one motor pair and switching-on of the other pair (t_{off_min}): > 500 [ms]

The typical requirement for the controlled system is that initial conditions and attitude perturbations shall asymptotically die away into a „well behaved" limit cycle. For the purpose of achieving appropriate performance, a tachometric feedback law and a first order compensator *C(s)* are added to the loop, resulting in the controlled system represented in Fig. 2.

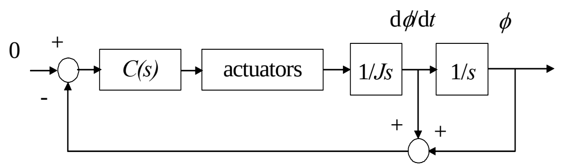

Fig. 2: Block diagram of the controlled system

The transfer function of the first order compensator is

$$C(s) = K\frac{s+z}{s+p}.$$

The goal in this contribution is to describe simulation-based investigations of the controlled systems behavior as a function of the controller parameters *p* and *z* and draw appropriate conclusions from the point of view of Control Engineering. A priori knowledge on this system is that, as long as the controller parameters satisfy the (approximate) limit cycle condition given by Oliveira and Kienitz (2000), limit cycle behavior is expected. If the condition is not satisfied, other types of persistent motion are expected. The limit cycle condition states that

$$t_{on\_min} + t_{off\_min} \le \frac{T}{2},$$

where *T* is the limit cycle period determined via a describing function approach from the intersection of the linear subsystem's Nyquist plot and the plot of $-1/N(\omega, A)$, with $N(\omega, A)$ being the non-linearity's describing function and $\omega = 2\pi/T$.

Simulation-based investigations will be consolidated in the form of bifurcation diagrams, as explained in section 4.

3. COMMENTS ON THE ACTUATOR MODEL

For simulation purposes, a second order transfer function will be used to model the actuator delay given in section 2. Thus the "actuator" block of Fig. 2 can be decomposed into a series structure with two sub blocks: the first one containing switching actuators and the second one containing linear second order dynamics which models the delays. In practice, actuator delays may vary during the operation of the system. Their value may depend on several parameters. Thus the model is affected by uncertainty. Such uncertainty will not be considered here. The overall actuator model used for simulation is depicted in Fig. 3.

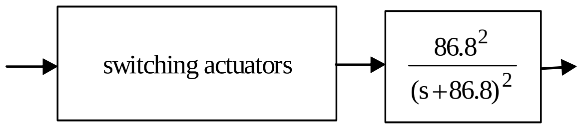

Fig. 3: Block diagram of the actuator model

4 – SIMULATION

The system of Fig. 2 (with the details in Fig. 3) was simulated using Matlab / Simulink and the xPC Target Tool (The MathWorks Inc., 2004) running on a master-slave two PC setup to achieve useful simulation performance. The switching logic was implemented as an S-function written in C. The controller was programmed in Simulink in such a way that controller parameters could be changed on the fly (i.e. in simulation time without recompilation). This demanded controller implementation using elementary Simulink functions, more specifically: summations, integrators and scalar gains. Thus the controller was implemented as follows:

$$C(s) = K\frac{s-z}{s-p} = K\left(1 + (p-z)\frac{1/s}{1-p\cdot 1/s}\right)$$

Although the xPC Target Tool is generally used for real-time simulation, it can also be used for „fastest possible" simulation. This was the option in our case.

The system was simulated on the slave PC for 1500 combinations of *p* and *z*. (Variations in *K* were not considered, because this parameter does not influence qualitative dynamic behavior.) The integration algorithm used was the implementation of a Runge-Kutta 4th-order method. The integration step chosen was 2 [ms]. Typical computation times are given on Table 1 for simulation of the same setup under Simulink/Windows and with xPC Target on the slave PC.

Table 1 – Comparison of simulators.

K = 1; z = -2.44; p = -11.1		
	Simulink	xPC Target
Simulated time *=70 [s]*		
Execution time	3.605 [s]	0.851 [s]
Maximum error	$9.5*10^{-16}$ [rad]	
Simulated time *=180 [s]*		
Execution time	11.326 [s]	1.773 [s]
Maximum error	$3.3*10^{-15}$ [rad]	

K = 2; z= -3; p = -20		
	Simulink	xPC Target
Simulated time *=70 [s]*		
Execution time	3.505 [s]	0.801 [s]
Maximum error	$1.9*10^{-15}$ [rad]	
Simulated time *=180 [s]*		
Execution time	11.166 [s]	1.712 [s]
Maximum error	$1.66*10^{-14}$ [rad]	

K =2; z = -30; p = -40		
	Simulink	xPC Target
Simulated time *=70 [s]*		
Execution time	3.505 [s]	0.782 [s]
Maximum error	$8.1*10^{-16}$ [rad]	
Simulated time *=180 [s]*		
Execution time	10.595 [s]	1.712 [s]
Maximum error	$9.1*10^{-16}$ [rad]	

Table 1 illustrates the advantage of the chosen simulation setup when compared to a Windows-only simulation. The line “maximum error” gives the maximum difference between both solutions (via Simulink and via xPC Target). The error is approximately equal to the available precision in xPC Target. Thus simulation using xPC Target was accepted for all subsequent analysis purposes.

Data were transferred from the slave to the master PC at the end of every simulation run with a decimation of 20, i.e. only every twentieth sample was transferred.

5 – RESULTS

Simulation results were consolidated into two types of bifurcation diagrams: diagrams of local maxima (Avanzini, 2001) and spectral bifurcation diagrams (Orrell and Smith, 2003). Both types of diagrams were prepared from the same data.

System behavior was simulated on the slave PC from 0 – 200 [s] for over 5600 combinations of p and z, with an integration step of 2 [ms]. Samples were sent to the master PC at every 40 [ms]. The spectral diagram demanded the computation of the fast Fourier transform (FFT), which was done on the master PC. From the available 5000 data points from every simulation, only the last 4096 were taken for fast FFT-computation. Thus initial transients were not considered.

A large amount of 2D diagrams was plotted. Two representative local maxima diagrams are given in Fig. 4 for $p = -3$; $-10 \leq z < 0$ and $p = -9$; $-10 \leq z < 0$. The spectral bifurcation diagrams for the same parameter values are shown in Fig. 5. It is seen that both types of diagrams allow for similar conclusions regarding bifurcation. For $p = -3$; $-10 \leq z \leq -4.2$ there is a limit cycle, while for higher values of z chaotic motion is present. For $p = -9$ there is chaotic motion in most of the considered range of z, except for two windows, slightly above and slightly below 5, where there is periodic motion. A similar analysis is possible using 2D diagrams throughout the range of parameters under consideration.

Switching attitude control systems have so far been operated in limit cycle mode. In such operation mode, initial conditions and attitude perturbations shall asymptotically die away into a “well behaved” limit cycle. This “good behavior“ of the limit cycle is usually defined in terms of an upper bound for attitude rate and maximum allowable attitude deviation. An approximate condition for the existence of limit cycles was derived by Oliveira and Kienitz (2000) for plants of the class considered in this article. If the condition is not satisfied, some other type of persistent motion is expected. With the help of the aforementioned condition, one approximate frontier for limit cycle behavior can be obtained. This frontier is indicated in black in Fig. 6.

The expression for the approximate bifurcation frontier is determined as follows. From Oliveira and Kienitz (2000) it is known that, in the scope of a describing function method setup, the maximum possible limit cycle frequency ω for the system in Fig. 2 is given by:

$$\omega = \pi / (t_{on\_\min} + t_{off\_\min}) \qquad (1)$$

A describing function for the switching actuators in Fig. 3 was derived by Oliveira and Kienitz (2000). As explained in that reference, this describing function can be decomposed into a (pure) time-delay-type phase shift and real valued function of limit-cycle frequency and amplitude. Define $M_g(\omega)$ as the *phase margin at frequency* ω of the linear subsystem in Figs. 2 and 3 including the aforementioned time delay, but excluding the controller. Within the approximation of the describing function method, limit cycle oscillation will occur with frequency ω, if the phase contribution of the compensator at that frequency equals M_g . The phase contribution of the compensator is determined from its frequency response

$$K \frac{j\omega - z}{j\omega - p} = K \frac{zp + \omega^2 + j\omega(z - p)}{\omega^2 + p^2}$$

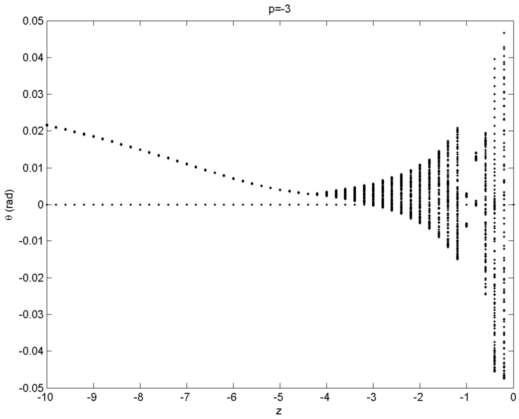

Fig. 4a: Diagram of maxima for *p* = -3.

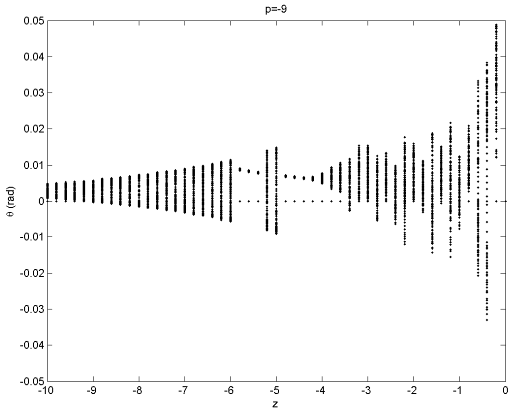

Fig. 4b: Diagram of maxima for *p* =-9.

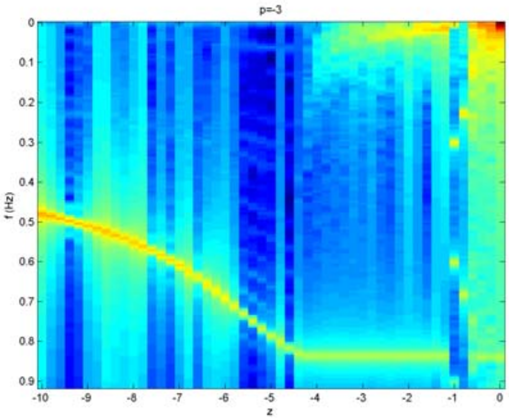

Fig. 5a: Spectral bifurcation diagrams for *p* = -3.

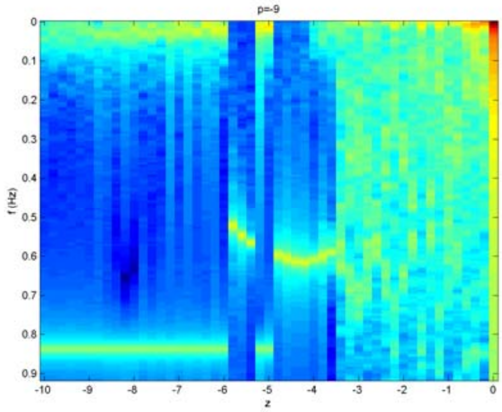

Fig. 5b: Spectral bifurcation diagrams for *p* =-9.

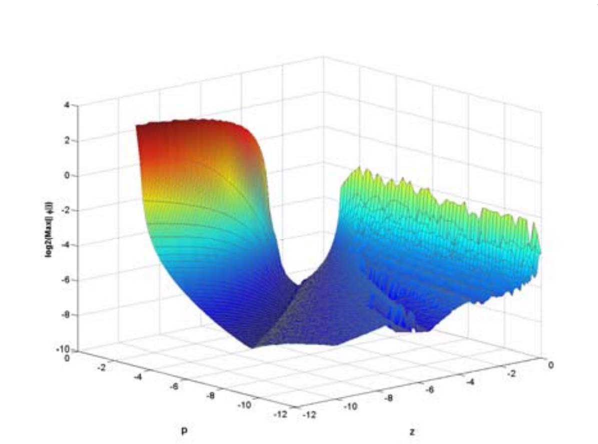

Fig. 6a: Three dimensional amplitude diagram.

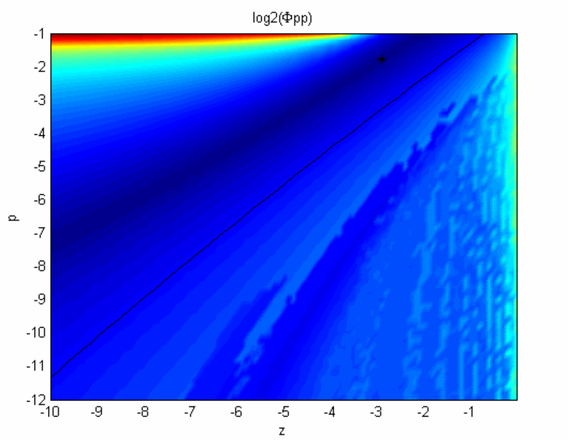

Fig. 6b: Projection of amplitude diagram on $p \times z$.

and is thus given by

$$tan^{-1}\left(\frac{\omega(z-p)}{zp+\omega^2}\right).$$

One approximate limit cycle frontier derived from a describing function approach is then defined by:

$$tan^{-1}\left(\frac{\omega(z-p)}{zp+\omega^2}\right) = M_g(\omega) \qquad (2)$$

with ω given by (1). Expression (2) defines the curve in the plane $p \times z$ that is plotted in black in Fig. 6.

Although limit cycle amplitude and frequency usually have been predicted with small acceptable errors using the describing function method, the black line in Fig. 6 is *not* a good approximation of the bifurcation frontier determined through simulation, given by the darkest region of the plot.

6 – CONCLUSIONS

It was shown that a variety of motions is possible in an attitude control system with switching actuators. From the point of view of control engineering it is interesting to know if quasi-periodic or chaotic persistent motions allow for smaller amplitudes than the “best possible” limit cycle. An inspection of Figure 6 leads to the conclusion that, in the case of the system considered herein, “best possible” behavior is attained in limit cycles near to the main bifurcation border. However, from an inspection of Figs. 4 and 5 it is seen that for combined frequency and amplitude specifications certain periodic windows away from the main bifurcation border may present interesting features for control. Further work will concentrate on this topic, as well as on the robustness of controlled systems that operate in such periodic windows or present chaotic motion.

The bifurcation border predicted via the describing function method and indicated as black solid line in Fig 6b is not a very good border approximation. Initial inquiries into the use of the (exact) Tsypkin method (Cook, 1986; Gelb and Velde, 1968) for the purpose of predicting bifurcation borders shows this to be a promising approach and additional work is being done on this issue.

ACKNOWLEDGEMENTS

The first author acknowledges support by FAPESP, Brazil (www.fapesp.br). The second author acknowledges partial support by FAPESP and the Alexander von Humboldt Foundation, Germany (www.avh.de).

REFERENCES

Avanzini, G. and Matteis, G. (2001) Bifurcation analysis of attitude dynamics in rigid spacecraft with switching control logics. *Journal of Guidance, Control, and Dynamics*, **24**, pp. 953-959.

Cook, P. (1986) *Nonlinear dynamical systems*. Prentice-Hall, Englewood Cliffs, N.J.

Gelb, A., and Vander Velde, W. (1968) *Multiple-input describing functions and nonlinear system design.* McGraw-Hill, New York.

Mendel, J. (1970) On-off limit cycle controllers for reaction-jet-controlled systems. *IEEE Trans. on Automatic Control*, **AC-15**, pp. 285-299.

Oliveira, N.M.F. and Kienitz, K.H. (2000) Attitude controller design for a system using actuators with switching-time restrictions and delays. *AIAA Guidance, Navigation, and Control Conference*, Paper AIAA-2000-3967, Denver.

Orrell, D. and Smith, L. (2003) Visualising bifurcations in high dimensional systems: The spectral bifurcation diagram. *Int. Journal of Bifurcations and Chaos*, **13**, pp. 3015-3027.

The MathWorks, Inc. *xPC Target 2.6.1 Product Description*, available from the internet address www.mathworks.com/products/xpctarget/.

Won, C. (1999) Comparative study of various control methods for attitude control of a LEO satellite. *Aerospace Science and Technology*, **5**, pp. 323-333.